Static Analysis of Contact Forces With a Mobile Manipulator

Bryan J. Thibodeau Patrick Deegan Roderic Grupen
Laboratory for Perceptual Robotics
Department of Computer Science
University of Massachusetts Amherst
Amherst, MA 01003
Email: {thibodea, pdeegan, grupen}@cs.umass.edu

***Abstract*— Most mobile robots in existence today have large, heavy, statically stable bases. To enable manipulation, actuated arms and effectors are attached to the base providing limited postural control. On the other hand, some of the latest developments in humanoid robotics have succeeded in reducing the footprint and raising the center of mass of a robot using whole body postural control and balancing. By comparing the magnitude of various forces that can be applied to the environment, we demonstrate the advantages of whole body postural control. The results presented suggest that for pushing, pulling, or carrying types of tasks, using whole body postural control can lead to higher performance by allowing a platform to apply more force to the environment.**

I. Introduction

In this paper, we focus on the effects of *whole body postural control* on the ability of a wheeled mobile manipulator to generate forces in static equilibrium. We define whole body postural control as the property of being able to control the angle of all links of the robot (including the base) relative to the ground. Under these conditions, we determine what forces at the end effector do not violate static stability.

We compare two similar planar wheeled mobile manipulators with 2-DOF arms. The orientation of the base of one robot is fixed so that it is perpendicular to the ground. The dynamically stable robot is free to orient its base with respect to the ground. The difference in the range of forces that each of these robots can apply at their end effectors is then determined. Since the robots are otherwise equivalent, the difference in performance is due exclusively to the effects of whole body postural control relative to limited postural control.

The robot model that we choose for this analysis is based on the uBot-4, a small wheeled bi-manual mobile manipulator, currently under construction. The statically stable configuration of this robot has four wheels, one pair at the front of the platform and one at the back. In a planar analysis, this reduces to two wheels, one at the front and one at the rear of the platform. The robot with whole body postural control will have just one pair of wheels in the middle of the platform and will balance around this set of wheels (much like a Segway® Human Transporter). Such a platform can perform whole body postural control by changing the angle of its base with respect to the ground.

II. Related work

There has been a significant amount of work on postural control for humanoid robots interacting with the environment. Khatib et al. (2003) [1] present a framework for performing tasks while maintaining postural constraints for a humanoid robot. In this work, the emphasis is on decoupling task and postural control rather than exploiting postural control to perform the task. Takubo et al. (2004,2005) and Harada and Kaneko (2003) [2][3][4] consider the control of a humanoid's posture during pushing tasks to ensure platform stability. In Yoshida et al. (2002) [5] a method is given to optimize the static posture of a humanoid robot with respect to an evaluation function that incorporates factors including force generation capabilities and the ability to reject disturbance forces. We use a similar method to determine static postures of the robot with whole body postural control. Harada et al. (2003) [6] consider the range of pushing forces that a humanoid robot can produce using whole body postural control. Hwang et al. (2003) [7] consider the magnitude of forces that can be dynamically generated by a humanoid robot for a variety of postures and physical properties of the robot. While these works characterize the force generation capabilities of robots using whole body postural control, they do not determine the gain in performance relative to a platform with limited postural control.

There are some examples of wheeled mobile robots that can control the posture of their bases, but to the authors' knowledge there have been no studies of wheeled mobile robots using postural control to accomplish manipulation tasks that would otherwise be impossible. Domains in which wheeled mobile manipulators have been employed include teleoperation for simulations of orbital manipulation tasks, [8], simple door opening tasks [8], and robot soccer [9]. None of these examples require whole body postural control to perform the tasks. Rather, dynamically stable bases are used because of their height, footprint, and agility. In this work we consider a dynamically stable base because it is a mechanically elegant platform for achieving whole body postural control with a wheeled mobile manipulator.

In the next section, we present a model of the robots used for evaluating the benefits of whole body postural control.

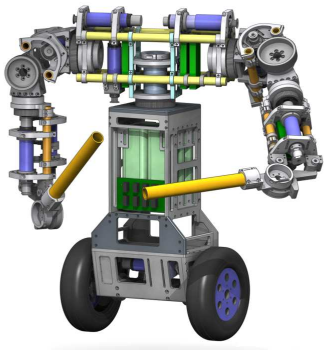

Fig. 1. Rendering of the uBot-4 design.

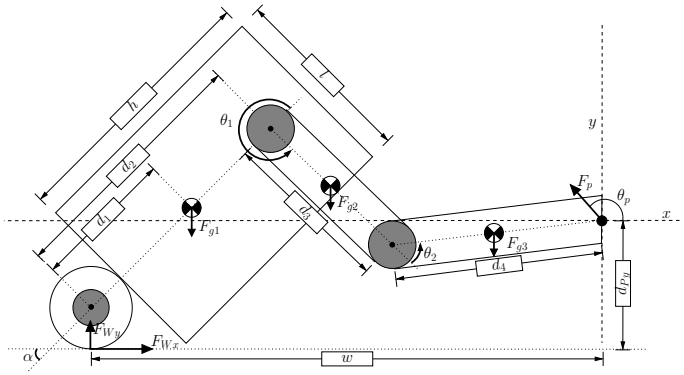

Fig. 2. Free body diagram of the platform with whole body postural control.

We then look at how different design choices affect the robots' ability to resist forces and introduce a simple metric to compare the force generation capabilities of two mobile manipulators. Lastly, we present an experiment demonstrating how whole body postural control can increase force generation capabilities.

III. Robot Model

The properties of our robot model approximate those of the uBot-4 (Figure 1), a platform which is currently under construction. The physical characteristics relevant to our analysis are (see Figure 2):

$h = 0.532$m	$d_3 = 0.262$m
$l = 0.240$m	$d_4 = 0.241$m
$r = 0.076$m	body$(m_1) = 6.163$Kg
$d_1 = 0.199$m	link 1$(m_2) = 2.644$Kg
$d_2 = 0.380$m	link 2$(m_3) = 0.314$Kg

Note that we assume that the robot's footprint is the smallest circle that circumscribes the robot's base. Thus, the value of l is very conservative since the the l for the uBot-4 is much smaller.

A free-body diagram of the posture controlled platform in a pushing configuration is shown in Figure 2. Note that the origin is at the end effector. For purposes of comparison, we assume that the statically stable version of the robot has a wheel in front and back, as in Figure 3, to provide the maximum possible stability given the width of the base. We assume that there is no difference in the robot's total mass or its distribution due to the difference in number or arrangement of wheels. $\mathbf{F_{g1}}$, $\mathbf{F_{g2}}$, and $\mathbf{F_{g3}}$ are the forces due to gravity on the body of the robot, the first link of the arm, and the second link of the arm respectively. F_{Wx} and F_{Wy} are the x and y components of the force exerted by the ground on the wheels. $\mathbf{F_p}$ is the force exerted on the end effector by the environment. We consider all possible values for θ_p such that $0 \leq \theta_p \leq 2\pi$.

We wish to determine the maximum magnitude of the force $|\mathbf{F_p}|$ in a given direction, θ_p. This is equal to the maximum $|\mathbf{F_p}|$ for which there is some configuration of the robot such that the robot is in static equilibrium and the force on the end effector is $|\mathbf{F_p}|$.

We consider the effect of friction between the wheels and the ground. μ is the coefficient of friction between the wheels and the ground, and slipping occurs when

$$|F_{Wx}| > \mu F_{Wy}. \tag{1}$$

In this work we assume $\mu = 0.5$.

For some positions and orientations of the force on the end effector, static equilibrium can be maintained for any value of $|\mathbf{F_p}|$. We therefore assume that there is some maximum force allowed at the end effector, $\overline{|\mathbf{F_p}|}$, due to joint torque limits or structural considerations.

Using Figure 2 we can find all of the moments that act around the wheel given the following values:

- w: The x-coordinate of the wheel;
- c: The x-coordinate of the center of mass of the robot body;
- s_x,s_y: The x, and y-coordinates of the robots shoulder (the first joint of the arm).

Also, assume the height at which the end effector is to make contact with the pushed object, d_{Py}, is given. Let g be the acceleration of gravity. The moment around the wheel, which must sum to zero in static equilibrium is:

$$\begin{aligned} &m_1 g(w-c) + m_2 g(w - 0.5(s_x + d_3\cos(\theta_1))) \\ &+m_3 g(w - ((s_x + d_3\cos(\theta_1) + 0.5 d_4 \cos(\theta_1+\theta_2)))) \\ &-d_{Py}|\mathbf{F_p}|\cos(\theta_p) - w|\mathbf{F_p}|\sin(\theta_p) = 0, \end{aligned} \tag{2}$$

Where $m_1 g(w-c)$, $m_2 g(w - 0.5(s_x + d_3\cos(\theta_1)))$, and $m_3 g(w - ((s_x + d_3\cos(\theta_1) + 0.5 d_4 \cos(\theta_1+\theta_2))))$ are the moments about the wheel due to the mass of the body, first link of the arm, and second link of the arm, respectively. The load at the end effector generates moments $-d_{Py}|\mathbf{F_p}|\cos(\theta_p)$, and $-w|\mathbf{F_p}|\sin(\theta_p) = 0$ about the wheel.

Solving for $|\mathbf{F_p}|$ yields:

$$\begin{aligned} |\mathbf{F_p}| \quad = \quad & (g(m_1(w-c) + m_2(w - 0.5(S_x + d_3\cos(\theta_1))) \\ & +m_3(w - (S_x + d_3\cos(\theta_1) \\ & +0.5 d_4 \cos(\theta_1+\theta_2))))) \\ & /(d_{Py}\cos(\theta_p) + w\sin(\theta_p)). \end{aligned} \tag{3}$$

The values of w, c, s_x, and s_y are computed for each type of robot below.

Since the robot is in static equilibrium, $|F_{Wx}| = |\mathbf{F_p}\cos(\theta_p)|$, and $|F_{Wy}| = m_t g - |Fp|\sin(\theta_p)$, where m_t is the total mass of the robot body and both links of the arms. Using Eq. 1, we find that the maximum value of $|\mathbf{F_p}|$ that does not break static friction is

$$|\mathbf{F_p}| = \frac{\mu m_t g}{|\cos(\theta_p)| + \mu \sin(\theta_p)}.$$

Note, that if $|\cos(\theta_p)| + \mu \sin(\theta_p) \leq 0$, then static friction will not be broken for any value of $|\mathbf{F_p}|$.

IV. Tipping conditions for platform with limited postural control

In the above analysis, we did not say how to control posture, i.e. how to determine w, c, s_x, or s_y, as these values are platform dependent. A free body diagram of the platform with limited postural control is shown in Figure 3. In static equilibrium w, the location of the ground reaction force, must be placed such that there is no net moment on the robot. This is called the zero moment point (ZMP)[10]. For any force on the end effector, the platform will not fall over if it can position itself such that the ZMP is between the front and back wheels. For the statically stable platform, w will always be the position of the ZMP.

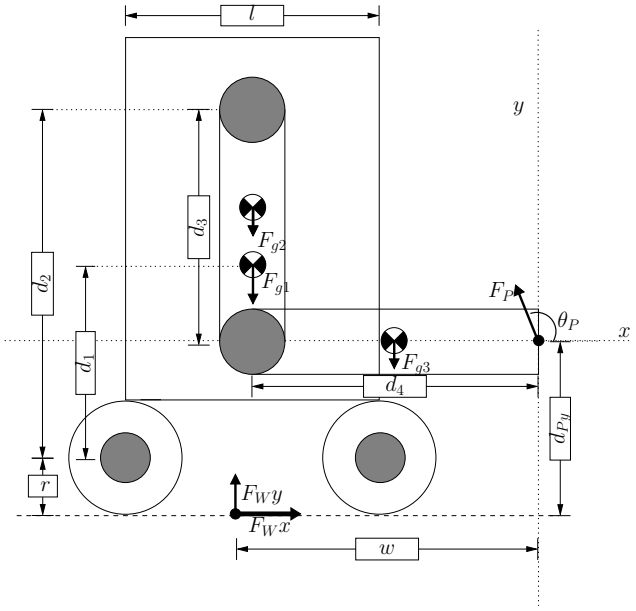

Fig. 3. Free body diagram of the platform with limited postural control.

Let $\underline{w}$ be the minimum possible position along the x-axis at which the leftmost wheel can be positioned given the endpoint position of its arm (note that the origin is to the right of the base). Let $\overline{w}$ be the maximum possible position along the x-axis at which the right wheel can be positioned. We will impose a constraint, $\underline{d_{Px}}$, on the minimum distance between the right edge of the robot's body and the end effector. This type of constraint might be used in a mobile manipulation application to ensure the robot's body does not collide with the manipulated object. In this paper, we assume that $d_{Px} = 0.05$m for all tasks. Figure 4 shows the relationship between $\underline{w}$ and $\overline{w}$. We can explicitly determine these values as:

$$\overline{w} = -\underline{d_{Px}}$$

$$\underline{w} = -\left(\sqrt{(d_3+d_4)^2 - (d_2 + r - d_{Py})^2} + l/2\right)$$

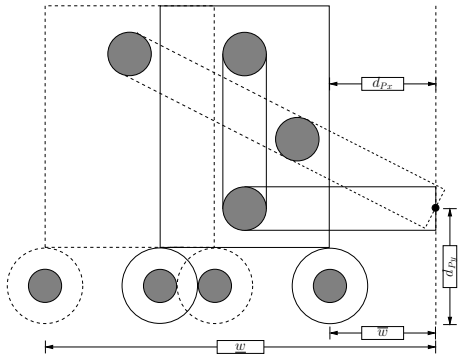

Fig. 4. The minimum and maximum values of w for which the statically stable platform can position it's support region over the ZMP.

If the line of action of $\mathbf{F_p}$ intersects the ground between $\underline{w}$ and $\overline{w}$, the platform will never tip over, since as $|\mathbf{F_p}|$ increases, the ZMP will tend toward the location where the line of action of $\mathbf{F_p}$ intersects the ground. Since the platform can place its support region over this point, it will not tip over no matter how large $|\mathbf{F_p}|$ becomes.

If the line of action of $\mathbf{F_p}$ intersects the ground to the left of the potential support region, then the maximum value of $|\mathbf{F_p}|$ that will not cause the platform to tip over is the value that causes the ZMP to be at the left edge of the potential support region. We can find this value of $|\mathbf{F_p}|$ using Eq. 3 with:

$$w = \underline{w} \tag{4}$$

$$c = \underline{w} + l/2 \tag{5}$$

Similarly, if the line of action of $\mathbf{F_p}$ projects to the right of the possible support region, we can find the maximum possible value for $|\mathbf{F_p}|$ using Eq. 3 with:

$$w = \overline{w} \tag{6}$$

$$c = \overline{w} - l/2 \tag{7}$$

In all of these situations we set s_x and s_y as follows:

$$s_x = c \tag{8}$$

$$s_y = d_2 + r - d_{Py}. \tag{9}$$

For situations where there are two possible configurations of the arm (elbow-up and elbow-down), we use the configuration that results in a higher value of $|\mathbf{F_p}|$.

V. Tipping Conditions for Platform with Whole Body Postural Control

The dynamically stable platform has an extra degree of freedom α, the angle between the body of the robot and the ground, as shown in Figure 2. In order for the dynamically stable platform to be in static equilibrium, the moment around the wheels must be zero. For a given value of θ_p, we can find the maximum value of $|\mathbf{F_p}|$ by solving for all of the terms in Eq. 3 in terms of w and α, and then numerically searching over the feasible combinations of w and α, choosing the combination that maximizes $|\mathbf{F_p}|$. For the dynamically stable platform:

$$\underline{w} = -d_2\cos(\alpha) - \sqrt{(d_3+d_4)^2 - (d_2\sin(\alpha) - d_{Py} + r)^2}, \tag{10}$$

and

$$\overline{w} = -(\underline{d_{Px}} + l/2). \tag{11}$$

Due to physical and control constraints on the angle between the platform and the ground, we assume $\pi/4 \leq \alpha \leq 3\pi/4$. For given values of w and d_{Py}, α must also obey the following constraints which ensure that the body of the platform is not too close to the end effector and that the point where the end effector is to make contact with the manipulated object is within the workspace of the manipulator:

$$\alpha \leq \cos^{-1}\left(\frac{d_2^2+w^2+(d_{Py}-r)^2-(d_3+d_4)^2}{2d_2\sqrt{w^2+(d_{Py}-r)^2}}\right) + \sin^{-1}\left(\frac{d_{Py}-r}{\sqrt{w^2+(d_{Py}-r)^2}}\right) \tag{12}$$

and

$$\alpha \geq \tan^{-1}\left(\frac{l/2}{h+r}\right) + \cos^{-1}\left(\frac{w-\underline{d_{Px}}}{\sqrt{(h+r)^2+(l/2)^2}}\right). \tag{13}$$

We can now solve for the variables in Eq. 3:

$$c = w + d_1\cos(\alpha), \tag{14}$$

$$s_x = w + d_2\cos(\alpha), \tag{15}$$

and

$$s_y = r + d_2\sin(\alpha) - d_{Py}. \tag{16}$$

Using Eqs. 3 and 10-16, it is straight forward to numerically approximate the maximum value of $|\mathbf{F_p}|$ which can be resisted by the platform in static equilibrium for a given θ_p. We consider both elbow-up and elbow-down configurations of the arm where appropriate.

We can now observe the performance of whole body postural control by comparing the force that can be applied/resisted by the end effectors of each robot. Figure 5 shows the maximum value of $|\mathbf{F_p}|$ as a function of θ_p for both types of platforms. We set $d_{Py} = 0.75m$. We can see that for a variety of directions, the platform with whole body postural control can withstand greater forces on its end effector.

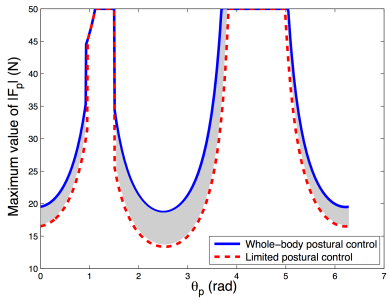

Fig. 5. Pushing force as a function of θ_p for the dynamically and statically stable robots with $d_{Py} = 0.75$m, $d_1 = 0.199$m, and $\overline{|F_p|} = 50$N. The shaded area indicates the area between the two curves. We use this area as a measure of the performance gain due to whole body postural control. The area between the curves is equal to 26.0[N·rad]

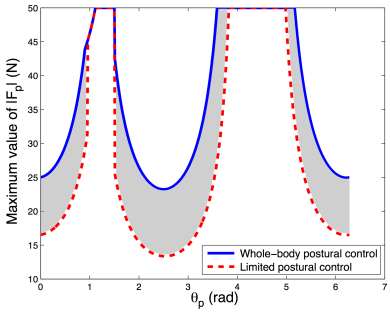

Fig. 6. Pushing force as a function of θ_p for the dynamically and statically stable robots with $d_{Py} = 0.75$m, $d_1 = 0.3$m, and $\overline{|F_p|} = 50$N. The area between the curves is equal to 52.9[N·rad]

VI. Analysis of Force Application/Resistance Capabilities

The ability of both the statically and dynamically stable robots to apply/resist a force at their end effectors is affected by the design of the robot and the location of the end effector. In this section, we examine how changing these parameters effects the relative performance of the two types of platforms.

As a simple scalar metric of the advantage of whole body postural control, we take the area between the curves generated by plotting force resistance as a function of θ_p for both versions of the robot in a given configuration (if the platform with limited postural control has a greater force generation capability for some values of θ_p, then we treat the difference between the two curves as "negative" area). Figures 5 and 6 demonstrate this metric for two different heights of the center of mass (d_1).

Figure 7 shows the advantage metric for whole body postural control of our platform as the mass of the robot is varied. There are two different effects that can be observed in this graph. The first is that when the mass is relatively low, the advantage of whole body postural control increases as total mass increases since larger forces/moments can be generated by moving the position of the center of mass. The second effect is that as the mass increases, both types of platform

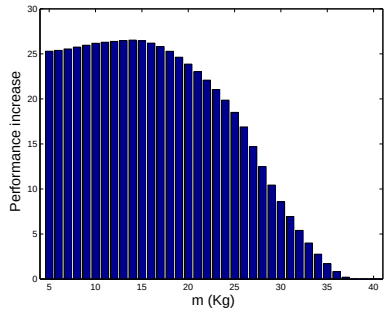

Fig. 7. Advantage of whole body postural control as a function of total mass. $d_{Py} = 0.75$ and $\overline{|F_p|} = 50$N.

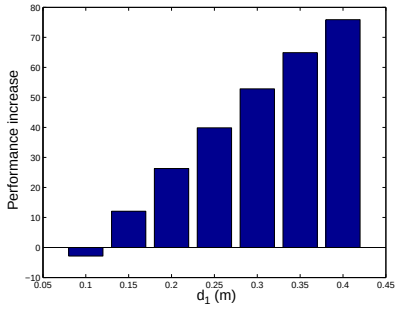

Fig. 8. Advantage of whole body postural control as a function of height of center of mass. $d_{Py} = 0.75$ and $\overline{|F_p|} = 50$N.

can withstand $\overline{|F_p|} = 50$N of force at the end effector in more directions. Thus, as the total mass becomes large the advantage of whole body postural control decreases until it is zero when both types of platforms can withstand $\overline{|F_p|} = 50$N in all directions.

Figure 8 demonstrates that the advantage of whole body postural control increases as the height of the platform's center of mass (d_1) increases. This is because as d_1 increases, whole body postural control allows the platform to move the center of mass over a greater range of positions, increasing the effectiveness of whole body postural control.

In Figure 9 the shaded region represents the force that the whole body postural controller can exert *in excess* of the force that limited postural control can exert in a given direction. It is important to note that θ_p is the direction of the force on the end effector, but in Figure 9 we are considering the force applied to the environment. For example, consider the direction indicated by the ray in Figure 9. The platform using whole body postural control can exert about 15N more in this direction than the platform with limited postural control. This direction corresponds to $\theta_p \approx \frac{5\pi}{4}$. Figure 10 shows the same analysis for a different height of the end effector.

These results suggest that platforms with whole body postural control excel, compared to statically stable platforms, at tasks that require manipulating large masses at a significant height. If a robot is to build, carry, or stack objects in an environment designed for a human, it needs to be able to

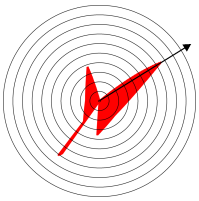

Fig. 9. Increase in forces that can be applied to the environment using whole body postural control, for $d_{Py} = 0.75$ and $\overline{|F_p|} = 50$N. Each concentric circle corresponds to a 2N increment, i.e. the platform using whole body postural control can apply ≈ 15N more in the direction indicated ($\theta_P \approx \frac{5\pi}{4}$) than the platform with limited postural control.

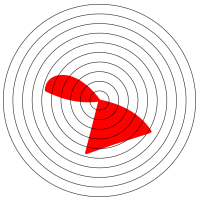

Fig. 10. Increase in forces that can be applied to the environment using whole body postural control, for $d_{Py} = 0.19$m and $\overline{|F_p|} = 50$N. Each concentric circle corresponds to a 2N increment.

manipulate heavy objects far from the ground without needing a footprint much larger than that of a human.

VII. Drawer Pushing Experiment

To demonstrate the advantage of whole body postural control, we performed a simple pushing experiment with our dynamically stable prototype robot, the uBot-3. We will not list the "as-built" properties of the uBot-3 here, but the main differences between the prototype and the uBot-4 design used in the rest of the paper is the total mass, which is 5.3Kg, and the height of the center of mass, measured from the wheel axle (d_2), which is 0.175m. In this experiment, the end effector is at a height of $d_{Py} \approx 0.48$m. To create a comparable statically stable robot without the capacity for whole body postural control, we added passive casters to the front and back of the robot as shown in Figure 12. This is not quite as stable a configuration as was analyzed earlier as the robot can tip around a point between a wheel and a castor. Figure 11 shows the predicted advantage of using whole body postural control for the task. The predicted advantage is not great for the uBot-3 as it is for the uBot-4. The predicted advantage of whole body postural control for pushing the drawer in ($\theta_p = \pi$) is only about 0.2N. For this reason, we believe that the forces arising from the dynamics of the postural change also contributed to the success in this experiment of the platform with whole body postural control.

A very simple pushing controller was implemented on each version of the platform. For the statically stable platform, once contact was made with the file cabinet, the torque at the wheels was increased until either a reference velocity was achieved (which would result in the drawer being closed) or a failure condition occurred (e.g. the robot fell over). A similar controller was implemented on the dynamically stable

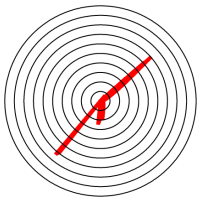

Fig. 11. Increase in forces that can be applied to the environment using whole body postural control using the uBot-3 prototype for $d_{Py} = 0.48$m and $\overline{|F_p|} = 50$N. Each concentric circle corresponds to a 1N increment.

platform which uses a linear quadratic regulator (LQR) to actively balance. The LQR takes a position reference as a control input. When the platform is in contact with a stationary object, the amount of force applied to the object can be controlled by altering the position reference. The LQR will cause the platform to take an appropriate posture to apply the desired force and no additional postural control is necessary for the pushing task.

Figure 12 shows the results of pushing a drawer filled with books using the above controllers with our prototype robot. The dynamically stable platform demonstrates an advantage of whole body postural control when it 'leans into' the drawer to overcome static friction. The statically stable platform is unable to move the drawer without tipping over.

VIII. Conclusion and Future Work

By comparing the magnitude of various forces that can be applied to the environment, we have demonstrated the advantages of whole body postural control. The results presented suggest that for pushing, pulling, or carrying types of tasks, a platform using whole body postural control is more efficient and effective since it can allow a given platform to apply more force to the environment without increasing the mass or footprint of the platform. In the future we plan to study similar problems accounting for dynamic effects. In addition to tasks requiring simple force application, we will study problems such as throwing and weight lifting. We expect to find even greater increases in the performance potential of the dynamically stable platform when dynamic effects are considered. We are constructing the uBot-4, a dynamically stable bi-manual mobile manipulator suitable for such experiments.

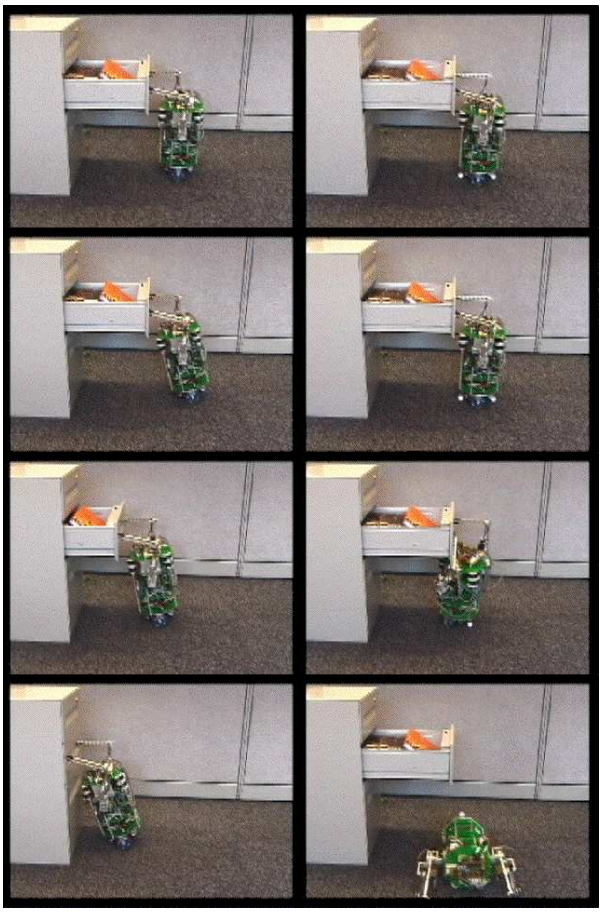

Fig. 12. The dynamically stable platform (left) and statically stable platform (right) pushing a drawer filled with books.

Acknowledgments

This work was supported in part by NASA/HRT/ASTP Contract #NNJ05HB61A. Any opinions, findings, conclusions, or recommendations expressed in this material are the author's and do not necessarily reflect those of the sponsors.

References

[1] O. Khatib, L. Sentis, J. Park, and J. Warren, "Whole body dynamic behavior and control of human-like robots," *International Journal of Humanoid Robotics*, 2003.

[2] T. Takubo, K. Inoue, K. Sakata, Y. Mae, and T. Arai, "Mobile manipulation of humanoid robots-control method for com position with external force," in *Proceedings of the 2004 IEEE/RSJ International Conference on Intelligent Robots and Systems*, Sendai, Japan, September 2004, pp. 1180–1185.

[3] T. Takubo, K. Inoue, and T. Arai, "Pushing an object considering the hand reflect forces by humanoid robot in dynamic walking," in *Proceedings of the 2005 IEEE International Confrence on Robotics and Automation*, Barcelona, Spain, April 2005, pp. 1718–1723.

[4] K. Harada, S. Kajita, K. Kaneko, and H. Hirukawa, "Pushing manipulation by humanoid considering two-kinds of ZMPs," in *Proceedings of the 2003 IEEE International Conference on Robotics and Automation*, Taipei, Taiwan, September 2003, pp. 1627–1632.

[5] H. Yoshida, K. Inoue, T. Arai, and Y. Mae, "Mobile manipulation of humanoid robots-optimal posture for generating large force based on statics," in *Proceedings of the 2002 IEEE International Conference on Robotics and Automation*, Washington, DC, 2002, pp. 2271–2276.

[6] K. Harada and M. Kaneko, "Whole body manipulation," in *Proceedings of the 2003 IEEE International Conference on Robotics, Intelligent Systems and Signal Processing*, Changasha, China, October 2003, pp. 190–195.

[7] Y. Hwang, A. Konno, and M. Uchiyama, "Whole body cooperative tasks and static stability evaluations for a humanoid robot," in *Proceedings of the 2003 IEEE/RSJ Intl. Conference on Intelligent Robots and Systems*, Las Vegas, Nevada, October 2003, pp. 1901–1906.

[8] H. G. Nguyen, J. Morrell, K. Mullens, A. Burmeister, S. Miles, nathan Farrington, K. Thomas, and D. W. Gage, "Segway robotic mobility platform," in *SPIE Proc. 5609: Mobile Robots XVII*, Philadelphia, PA, October 2004.

[9] B. Browning, P. E. Rybski, J. Searock, and M. M. Veloso, "Development of a soccer-playing dynamically-balancing mobile robot," in *Proceedings of the 2004 IEEE International Conference on Robotics and Automation*, New Orleans, LA, April 2004, pp. 1752–1757.

[10] M. Vukobratović, A. A. Frank, and D. Juričić, "On the stability of biped locomotion," *IEEE Transactions on Biomedical Engineering*, vol. 17, no. 1, pp. 25–36, 1970.